

Channel Capacity Enhancement by Pattern Controlled Handset Antenna

Hiroyuki ARAI, Junichi OHNO

Yokohama National University, Department of Electrical and Computer Engineering,
79-5 Tokiwadai, Hodogaya-ku, Yokohama-shi, Kanagawa, Japan

arai@ynu.ac.jp

Abstract. This paper presents a radiation pattern controlled antenna for handset terminals to reduce the correlation coefficient between antennas and enhance the channel capacity in MIMO applications. A pair of small inverted-F shaped antennas combined by a phase shifter provides a single port with controlled pattern. To enhance the channel capacity, the phase difference for the IFA array is optimized using the evaluation parameter of reception level, correlation coefficient and mean effective gain of the proposed array geometry. The channel capacity enhancement is verified by assuming Croneker scattering under Nakagami-Rice propagation model.

Keywords

MIMO, inverted-F shaped antenna, channel capacity, correlation coefficient, MEG.

1. Introduction

In the upcoming cellular phone service, high speed data transmission is expected and MIMO (Multiple Input and Multiple Output) system is a key technology. The number of antennas is required to increase the channel capacity [1], [2]. However, a handset has many built-in antennas for other applications in addition to the cellular service. To enhance the channel capacity for small number of antenna systems, the spatial correlation between antenna elements should be decreased. A multi-receiver increases the circuit complexity and power consumption in the digital signal processing unit, while a decrease of the number of antennas provides simple receiver design on the contrary. A solution for this conflicting problem is an analog antenna pattern control [3]. Phased array antennas, conventionally used in many applications, change only input signal weights by the phase shifters. Recently, small and low cost analog phase shifters are commercially available by the progress of integrated filter technologies [4]. To simplify the feeding circuit, a fixed phase difference by delay lines is also useful.

This paper presents an antenna with adaptive pattern controlled by the analog phase shifter. Selecting the opti-

imum phase difference results in the channel capacity enhancement for the MIMO system. This is verified by simulating the antenna performance using a Nakagami-Rice propagation model. The criterion to select the optimum phase difference, we use the reception level, MEG (Mean Effective Gain) and correlation coefficient between antennas.

2. Multi-Antenna for Handset

Small Inverted F-shaped wire antennas (IFA) are mounted on the top of conducting box imitating a handset terminal as shown in Fig. 1. As reference arrays, an orthogonal and a parallel arrangements of antenna element are prepared. The IFA parameters and array geometries are also shown in Fig. 1, where the IFA parameters are optimized to resonate at 3.8 GHz, the frequency band for high data wireless transmission. The antenna consists of conducting wires with the diameter of 1 mm. The shorting pin of IFA is adjusted to suppress the S_{11} less than -10 dB and this geometry is used throughout the paper. The S_{21} is less than -11 dB for the parallel array and -14 dB for the orthogonal array, which are small enough for the handset antenna. The antenna characteristics in this paper are calculated by FEKO [5].

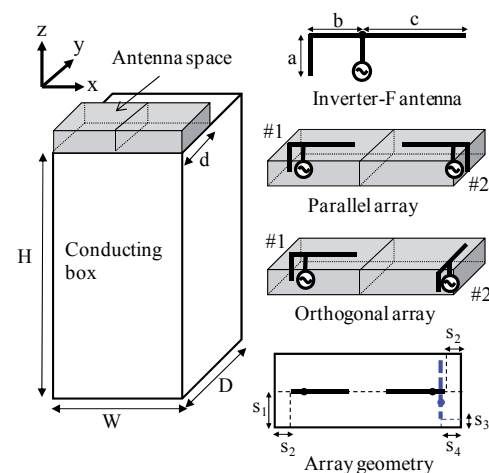


Fig. 1. Geometry of handset antenna, $H=100$, $W=50$, $D=20$, $d=10$, $a=7$, $b=1.5$, $c=13$, $s_1=10$, $s_2=s_4=2$, $s_3=s_5=1.5$, (mm).

To control the antenna radiation pattern, a pair of IFAs excited with some phase differences is replaced with the antenna element in Fig. 1. The feeding circuits are shown in Fig. 2 for the parallel array and the array 2 is replaced by the elements denoted as dotted lines for the orthogonal array. The mutual coupling between IFA elements is less than -10 dB for both arrangements. The element spacing of 0.13λ at 3.8 GHz increases the mutual coupling to -7 dB, when the antennas are on the infinite ground plane. The antenna position near the box edge improves the mutual coupling by 3 dB.

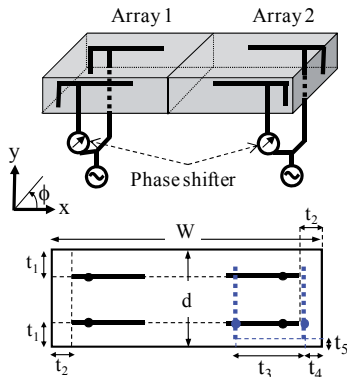


Fig. 2. Geometry of array by pairs of IFAs, $W=50$, $d=20$, $t_1=5$, $t_2=t_4=2$, $t_3=15$, $t_5=1.5$ (mm).

A typical radiation pattern of reference antenna #1 in Fig. 1 is shown in Fig. 3. The pattern in the xy plane has the maximum gain to the x axis ($\phi=0$), because of the current flowing on the conducting box. The pattern of #2 is given by rotating 180° of those of #1. The pattern of array will be discussed later.

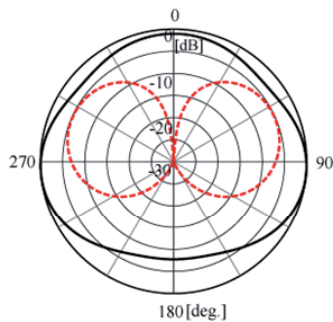


Fig. 3. Radiation pattern in xy plane of reference antenna #1. Solid line is vertical polarization, and dotted line is horizontal polarization.

3. Phase Controlled Pattern

As an ideal approach, the optimum phase difference for the IFA array is changed adaptively based on the fluctuation of propagation environment. A simple approach for the phase control should be developed to obtain low cost antenna systems. A fixed phase difference or small number of phase switching is appropriate for the handset, then we examine the phase difference to increase the antenna gain.

This criterion is given by evaluating the reception signal level for a plane wave incidence with some angles in the xy plane. We change the phase difference from 0° to 360° for the fixed angle of plane wave incidence.

Fig. 4 shows the output reception level of array #1 in Fig. 2. Since the array #1 and #2 are symmetrical, only the reception level of #1 is presented, where four incident angles in the xy plane are examined. The output level of array #1 is given by changing the phase difference of antenna element, where an ideal phase shifter without insertion losses is assumed. The incident angles are $\phi_i=0^\circ, 90^\circ, 180^\circ$ and 270° . The array geometry is symmetrical about the x axis, then the curves in Fig. 4 are symmetrical to the phase difference of $\delta=180^\circ$. The maximum reception levels are obtained at $\delta=\pm 30^\circ$ for $\phi_i=90^\circ$ and 270° , and $\delta=0^\circ$ for $\phi_i=0^\circ$ and 180° . In these examples of incident angles, three phase differences are selected to obtain high reception level. The phase switching may be selected to maximize the reception level, for example, as RSSI (Receive Signal Strength Indication).

The same evaluations are given for the orthogonal array which is given by replacing array #2 with dotted lines in the bottom in Fig. 2. The reception level by #1 is almost same with Fig. 4, then the reception levels are shown for the array #2 as shown in Fig. 5. The optimum phase differences are $\delta=\pm 30^\circ$ for $\phi_i=0^\circ, 90^\circ, 180^\circ$, and $\delta=60^\circ$ for $\phi_i=270^\circ$. In this array arrangement, the phase switching also increases the reception level for four incident angles. To discuss the increase of reception level in more detail, we evaluate the channel capacity for MIMO application using several propagation models in the following.

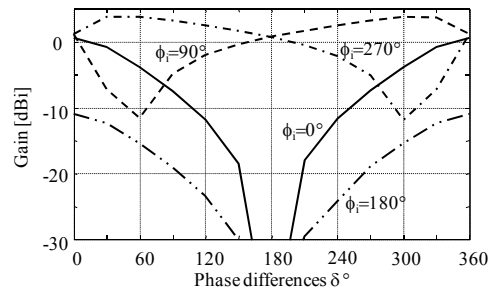


Fig. 4. Reception level of parallel array by pairs of IFAs as a function of phase difference for 4 incoming waves.

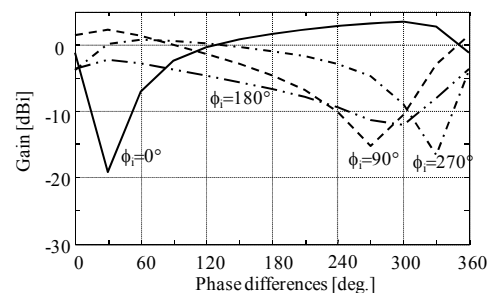


Fig. 5. Reception level of orthogonal array by pairs of IFAs as a function of phase difference for 4 incoming waves

4. Channel Capacity for MIMO

For the diversity application, the orthogonal polarization is effective to reduce the correlation coefficient between two antenna ports, however, the channel capacity of MIMO also depends on the antenna gain. To examine the phase control effect for MIMO applications, this section presents the channel capacity of these arrays. The propagation model used in this paper is a Nakagami-Rice propagation model together with Croncker scattering assumption by the surroundings [6]. For the simplicity in the simulation, we assume all the incoming waves are concentrated in the xy plane and channel matrix is presented as follows,

$$\mathbf{H}(\phi) = \sqrt{\frac{K}{K+1}} \mathbf{H}_D(\phi) + \sqrt{\frac{1}{K+1}} \mathbf{H}_S \quad (1)$$

where \mathbf{H}_D and \mathbf{H}_S are direct and scattering components and ϕ is the angle of incident wave in the xy plane [7].

$$\mathbf{H}_D(\phi) = \Gamma(\phi) \circ \mathbf{a}(\phi), \quad \mathbf{H}_S(\phi) = \mathbf{R}_r^{1/2} \mathbf{G}(\mathbf{R}_t^{1/2})^t \quad (2)$$

$\Gamma(\phi)$ and $\mathbf{a}(\phi)$ are complex radiation pattern of each antenna and array factor, and \circ represents the Hadamard product. \mathbf{G} is Gaussian distribution matrix and the correlation matrix at reception side \mathbf{R}_r is given as,

$$\mathbf{R}_r = \begin{pmatrix} P_{r1} & \sqrt{P_{r1}P_{r2}}\rho \\ \sqrt{P_{r1}P_{r2}}\rho & P_{r2} \end{pmatrix} \quad (3)$$

where P_{ri} ($i=1, 2$) is the reception power and ρ is the correlation factor between output ports. The correlation matrix at transmission side \mathbf{R}_t is a unit matrix and superscript t denotes transport matrix. The transmitted signals are uncorrelated with the same power level.

We calculate the channel capacity for these arrays by the above channel matrix as [8],

$$C(\phi) = \sum_{l=1}^2 \log_2 \left(1 + \frac{\gamma \lambda_l(\phi)}{M} \right) \quad (4)$$

where γ is Signal to Noise Ratio (SNR), and λ is eigenvalue of each mode. The number of transmission antenna M is 2 and the SNR is 20 dB, and Ricain factor is 3 dB throughout this paper.

Fig. 6 shows the channel capacity of IFA arrays under the propagation model described above. The horizontal axis represents the angle of incoming direct wave from the transmitter. The solid and dashed curves are the capacity of IFA array without phase control as shown in Fig. 1. The reception level is given as a sum of each output port of IFAs. The orthogonal array in Fig. 1 has higher capacity for most of the incident angles except for the $250^\circ < \phi_i < 340^\circ$. The channel capacity enhancement by phase controlled array is also shown in Fig. 6, where we select two phase difference combination $(\delta_1, \delta_2) = (-60^\circ, +60^\circ)$ and $(+60^\circ, -60^\circ)$ for the orthogonal array as shown in Fig. 2. The δ_1 and δ_2

are the phase difference of array #1 and #2, respectively. These phase differences of $\delta = \pm 60^\circ$ are selected to provide large reception level given by the results as in Fig. 5. The $\delta = \pm 60^\circ$ provide the maximum reception levels for $\phi_i = 90^\circ$ and 270° , while it reduces the level by 5dB for $\phi_i = 0^\circ$ and 180° from their maximums. A fine phase control is preferable to maximize the reception levels, however, the minimum number of phase switching is tried in this example. By these phase combinations, the reception level is enhanced compared with the IFA array without phase control.

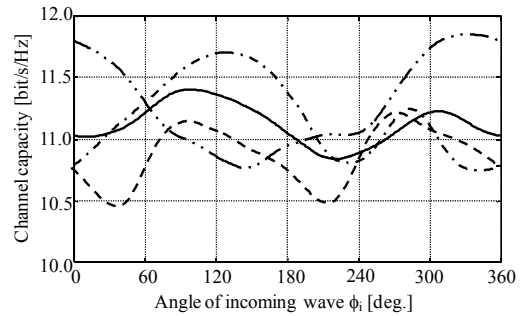


Fig. 6. Channel capacity of IFA array w/ and w/o phase control, solid line is orthogonal array and dashed line is parallel array in Fig. 1, - . - : $\delta_1 = -60^\circ, \delta_2 = +60^\circ$, . . . : $\delta_1 = +60^\circ, \delta_2 = -60^\circ$ for Fig. 2.

As shown in Fig. 6, two capacity curves of two phase combinations for the array in Fig. 2 are crossing at $\phi_i = 60^\circ$ and 200° . When we switch the phase difference at these incoming wave angles, high channel capacity is expected for this array configuration. This procedure is applied to the parallel and orthogonal array in Fig. 2, then both of channel capacities are compared in Fig. 7. The phase difference of $\delta = \pm 30^\circ$ is selected for the parallel array, because this phase difference provides the maximum reception level in the results in Fig. 4.

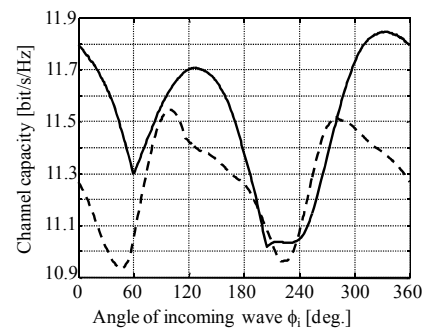


Fig. 7. Channel capacity of orthogonal (solid line) and parallel (dotted line) array w/ phase switching, $\delta = \pm 30^\circ$ for parallel array and $\delta = \pm 60^\circ$ for orthogonal array.

The radiation pattern of these array elements are shown in Figs. 8 and 9. The switched pattern in each array element is symmetrical, which is a good choice for the phase switching. The capacity of orthogonal array is higher than the parallel array except for the incident angle around $\phi_i = 240^\circ$, however high capacity is obtained for most of the

incident angles. These phase selection is based on a simple evaluation factor by the reception level of each array element as shown in Figs. 4 and 5. We do not have clear criterion to select these phase differences and their switching methods. To show a distinct phase selection scenario, we investigate the MEG and correlation factor between antenna output ports in the next section.

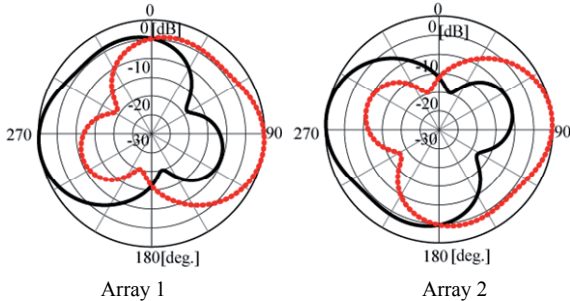


Fig. 8. Radiation pattern of vertical polarization in xy plane for parallel array, solid line is $\delta = +30^\circ$, and dotted line is $\delta = -30^\circ$.

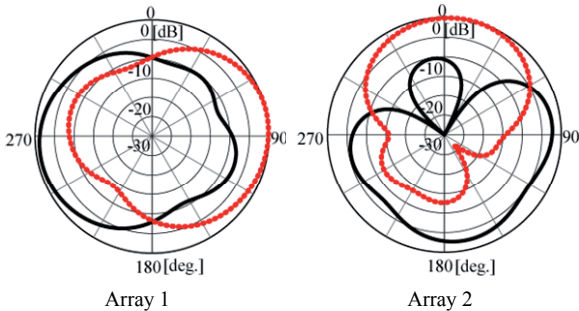


Fig. 9. Radiation pattern of vertical polarization in xy plane for orthogonal array, solid line is $\delta = +60^\circ$, and dotted line is $\delta = -60^\circ$.

5. MEG and Correlation Coefficient

As an evaluation parameter, the correlation coefficient between two output ports is obtained by the complex radiation pattern in the xy plane. Another parameter by the sum of MEGs [9] is also introduced here. We obtain two MEG values for two output ports in the array geometry of Fig. 2, then we simply add two MEG values for the evaluation factor. This criterion is equivalent to the sum of RSSI levels by the two receivers. The incident wave model is the same with Section 4, and we only use the incident wave angle at $\phi_i = 0^\circ$ for the simplicity in calculation. The orthogonal array geometry in Fig. 2 is evaluated in the following, because it provides higher capacity.

The correlation coefficient between two output ports as a function of phase difference δ for each array element is shown in Fig. 10. Two phase combinations as out of phase ($\delta_1 = -\delta_2$) and in-phase ($\delta_1 = \delta_2$) are examined here. Each case takes the minimum of the correlation coefficient at $\delta = 150^\circ, 300^\circ$. They are marked by small squares in Fig. 10. The sum of MEGs is also shown in Fig. 11, where it takes the maximum at $\delta = 150^\circ, 270^\circ$. The out of phase

case takes the same phase difference to optimize the correlation and MEG, however, it has a slight difference for in-phase case. To find the better choice for the criterion to enhance the channel capacity, Fig. 12 shows the capacity as a function of all the incoming wave directions for the phase difference selected by the reception level, the correlation coefficient and the sum of MEGs. For the reference, the capacity of no phase difference $\delta = 0^\circ$ is also shown.

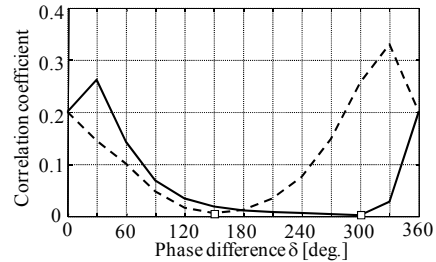


Fig. 10. Correlation of orthogonal array by pairs of IFAs as a function of phase difference, $\delta_1 = \delta_2$ for solid line, $\delta_1 = -\delta_2$ for dotted line

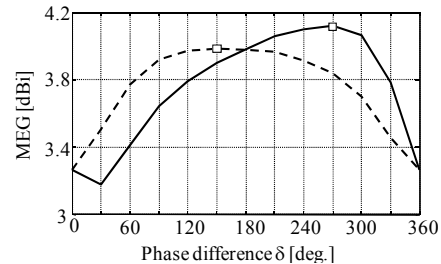
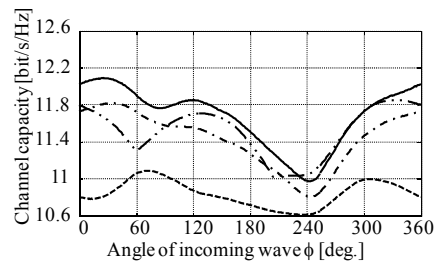
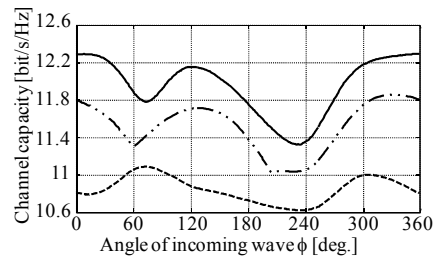


Fig. 11. Sum of MEGs for orthogonal array by pairs of IFAs as a function of phase difference, $\delta_1 = \delta_2$ for solid line, $\delta_1 = -\delta_2$ for dotted line.



(a) In-phase case, solid line is $\delta_1 = \delta_2 = 270^\circ$ by Fig. 11, \dots is $\delta_1 = \delta_2 = 300^\circ$ by Fig. 10, $-\cdot-\cdot-$ $\delta_1 = \delta_2 = \pm 60^\circ$ by Fig. 7.



(b) Out of phase case, solid line is $\delta_1 = -\delta_2 = 150^\circ$ by Figs. 10 and 11, \dots $\delta_1 = \delta_2 = \pm 60^\circ$ by Fig. 7.

Fig. 12. Channel capacity with phase selection by MEG and correlation, dashed line is $\delta_1 = \delta_2 = 0^\circ$.

In-phase case, the optimum phase selected by the sum of MEGs provides high channel capacity for all the incoming angles as in Fig. 12 (a), though the MEG is calculated only for $\phi=0^\circ$. The out of phase case takes the same optimum phase difference by the correlation and the sum of MEGs as in Fig. 12 (b). The average channel capacity enhancement is 10 % by this optimum phase selection.

The above results show that the phase controlled IFA array provides high channel capacity for the handset antennas. The propagation model of incident wave has no correlation between direct and scattered waves in the above discussion. For example, the correlation factor of 0.3 in out of phase case decreases the maximum value of channel capacity by 5%, however, the capacity curves are the same with Fig. 12 (b). In addition, the channel capacity of the orthogonal IFA array with the same phase difference in Fig. 12 is shown by using the incoming wave with the angular spread of 12° as typical examples [10]. The absolute value of channel capacity depends on the propagation model, however the proposed phase control method provides higher channel capacity for this propagation model. These results show that the proposed criterion to select phase difference increases the channel capacity without loss of generalities.

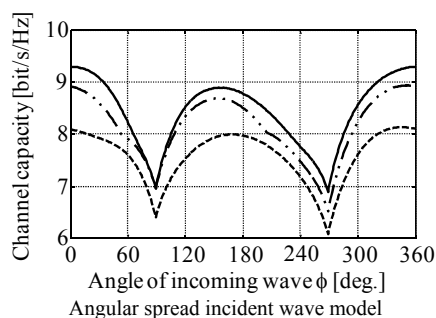


Fig. 13. Channel capacity of orthogonal IFA array by out of phase difference, solid line is $\delta_1 = -\delta_2 = 150^\circ$ by Figs. 11, --- $\delta_1 = \delta_2 = \pm 60^\circ$ by Fig. 7 and dashed line is $\delta_1 = \delta_2 = 0^\circ$.

6. Conclusions and Discussions

This paper presented pattern controlled IFA arrays using analog phase shifter for the handset antenna applications. To enhance the channel capacity, the phase difference for the IFA array is optimized using the evaluation parameter of the reception level, the correlation coefficient and the mean effective gain of the proposed array. The channel capacity enhancement was obtained by selecting the phase difference to minimize the correlation coefficient or to maximize the sum of MEGs. These simple phase selection is very effective to apply the handset antenna.

This paper presented basic idea to select the optimum phase difference for small antenna arrays, and did not show real switching circuits. The best solution is a fixed phase

difference by delay line, because the analog phase shifter has insertion losses to decrease the channel capacity. The phase controlled antenna should be tested in real propagation environment in addition to the effect of body and hands, which is left for the future problems.

References

- [1] NIRMAL KUMAR DAS, TAKASHI INOUE, TETSUKI TANIGUCHI, YOSHIO KARASAWA An experiment on MIMO system having three orthogonal polarization diversity branches in multipath-rich environment. *Proc. IEEE VTC 2004-Fall*, Sep. 2004.
- [2] GETU, B. N., ANDERSEN, J. B. The MIMO cube - a compact MIMO antenna. *IEEE Trans. Wireless Comm.*, May 2005, vol. 4, no. 3, pp. 1136-1141.
- [3] AOYAMA, H., ARAI, H. Mutual coupling matrix estimation and null forming methods for MBF antennas. *Trans. IEICE Japan*, vol.E88-B, Jun.2005, no.6, pp.2305-2312.
- [4] SEUNG-WOOK NAH, ARAI, H. Beam-space MUSIC DOA system using phase shifter. *Trans. IEICE Japan*, Feb.2007, vol.E90-B, no.2, pp.291-295.
- [5] www.feko.info
- [6] KERMOAL, J. P., SCHUMACHER, L., PEDERSEN, K. I., MOGENSEN, P. E., FREDERIKSEN, F. A stochastic MIMO radio channel model with experimental validation. *IEEE Journal on Selected Areas in Communications*, Aug. 2002, vol.20, no.6, pp.1211-1226.
- [7] MAKOTO TSRUTA, YOSHIO KARASAWA Simplified estimation method of the largest eigenvalue distribution in Nakagami-Rice MIMO channel. *IEICE Trans-B*, Sept. 2004, vol. J87-B, no. 9, pp. 1486-1495 (in Japanese)
- [8] TAKEO OHGANE, TOSHIHIKO NISHIMURA, YASUTAKA OGAWA Applications of space division multiplexing and those performance in a MIMO Channel. *Trans. IEICE Japan*, May 2005, vol.E88-B, no. 5, pp. 1843-1851.
- [9] TAGA, T. Analysis for mean effective gain of mobile antennas in land mobile radio environments. *IEEE Trans. Vehicular Technology*, May 1990, vol. 39, no. 2, pp. 117-131.
- [10] KARASAWA, Y. Statistical multipath propagation modelling for broadband wireless systems. *Trans. IEICE Japan*, Mar. 2007, vol.E90-B, no.3, pp.468-484.

About Authors

Hiroyuki ARAI was born in Ibaraki, Japan. He received his M. Eng. and Phd. from Tokyo Institute of Technology in 1984 and 1987, respectively. He is now professor at Yokohama National University. His research interests include mobile antenna system, antenna measurement and DOA.

Junichi OHNO was born in Tokyo, Japan. He is a graduate student at Yokohama National University and his research interest is MIMO antennas.